Journal of Computational Physics 299 (2015) 229–280

Contents lists available at ScienceDirect

Journal of Computational Physics

www.elsevier.com/locate/jcp

Reduction of dissipation in Lagrange cell-centered hydrodynamics (CCH) through corner gradient reconstruction (CGR)

D.E. Burton *, N.R. Morgan, T.C. Carney, M.A. Kenamond

X-Computational Physics Division, Los Alamos National Laboratory, P.O. Box 1663, Los Alamos, NM, USA

ARTICLE INFO

Article history:
Received 8 January 2015
Received in revised form 15 June 2015
Accepted 24 June 2015
Available online 8 July 2015

Keywords:
Lagrangian
Hydrodynamics
Godunov
Cell-centered
Finite-volume
Reconstruction
Higher-order
Dissipation
CCH
Corner gradient reconstruction
CGR

ABSTRACT

This work presents an extension of a second order cell-centered hydrodynamics scheme on unstructured polyhedral cells [13] toward higher order. The goal is to reduce dissipation, especially for smooth flows. This is accomplished by multiple piecewise linear reconstructions of conserved quantities within the cell. The reconstruction is based upon gradients that are calculated at the nodes, a procedure that avoids the least-square solution of a large equation set for polynomial coefficients. Conservation and monotonicity are guaranteed by adjusting the gradients within each cell corner. Results are presented for a wide variety of test problems involving smooth and shock-dominated flows, fluids and solids, 2D and 3D configurations, as well as Lagrange, Eulerian, and ALE methods.

1. Introduction

In cell-centered hydrodynamics schemes (CCH), all conservation equations are solved on a common control volume. As we discuss later, modern CCH methodology was enabled by the work of Després and Mazeran [33], followed by Maire and others [74,13]. The following work is based upon the particular second order method (denoted CCH2) described in [13,15], but the results are applicable to other implementations.

As discussed in [13] and also in [16], CCH is quite accurate on shock-driven test problems. However, it has been noted that the second order method can generate dissipation errors for many smooth flows. As an example of the dissipation, we consider the motion of an oscillating elastic plate that will be discussed in detail in Section 5.1. Fig. 1 shows the calculated vertical velocity of the central point of the plate. Because the plate is elastic, the amplitude of the oscillations should remain relatively constant in time. For an undamped reference calculation (green), this is essentially true. However, the CCH2 method artificially dissipates kinetic energy.

In this work, we seek to increase the accuracy of CCH by employing a higher order extension that significantly reduces the dissipation error in such cases. CCH2 uses a finite volume spatial integration and a two stage Runge–Kutta temporal

* Corresponding author.
E-mail address: burton@lanl.gov (D.E. Burton).

http://dx.doi.org/10.1016/j.jcp.2015.06.041
0021-9991/

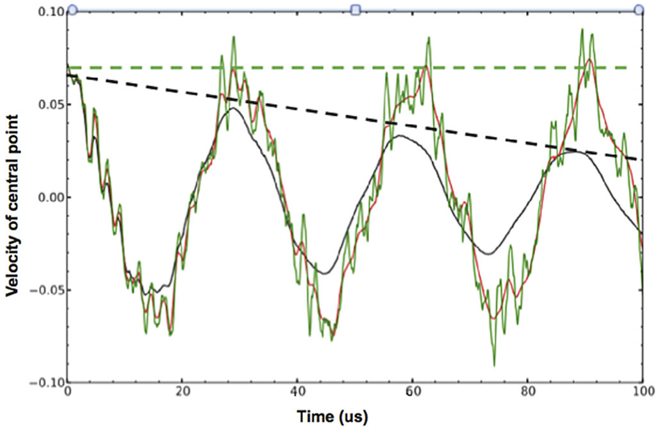

Fig. 1. Vertical velocity of the central point in a bending Be plate. Reference calculation (green), CCH2 (black), (red) to be discussed later. (For interpretation of the references to color in this figure legend, the reader is referred to the web version of this article.)

integration (RK2). Each Lagrange step begins with the knowledge of the extensive values of conserved quantities within cells. In finite volume methods, the distribution of conserved quantities within a cell is not known *a priori* and must be "reconstructed" or inferred from values in adjacent cells. As described later, 2nd and higher order CCH methods differ principally in the details of this reconstruction that must be constrained to be both conservative and monotonic. In the 2nd order reconstruction of Refs. [13,71], conserved quantities within cells are distributed linearly using monotonicity preserving gradients. A 3rd order reconstruction would require a quadratic polynomial having 6 coefficients in 2D and 10 in 3D. A least-squares (LSQ) solution for those coefficients involves the computationally expensive solution of a multi-equation system for each cell and for each reconstructed variable. Further, as discussed by Cheng and Shu [27], third and higher order schemes require curvature of the cell faces to achieve the specified order. Our work focuses on improvements to the second-order method while retaining straight cell faces.

A more computationally efficient alternative to 3rd order is a piecewise linear reconstruction that we call Corner Gradient Reconstruction or CGR. The method is not formally 3rd order, but captures many of its properties. In CGR, linear functions are generated at each mesh point and applied in each cell corner. The solution for the point gradients involves only Cramer's rule.

1.1. Organization of the paper

The paper is organized in two principal parts, the first explaining the theory and the second presenting test calculations. The theory begins with a brief explanation of notation in Section 1.2 and follows with an overview of CCH2 in Section 2. The notion of reconstruction is explored generally in Section 3 and in detail for CGR in Section 4. The test problems beginning in Section 5 are ordered by (a) smooth flows starting in Section 5.1, (b) shock dominated flows starting in Section 6.1, (c) and finally Eulerian and ALE problems starting in Section 7.2. We summarize our conclusions in Section 8. Details of the solid model are given in Appendix A.

1.2. Mesh topology and notation

A discretization stencil describes how information defined on grids is spatially connected. It is important that the mathematical formulation be consistent with the stencil. For polytopal grids, potential complexity is overcome by finding a simple but universal stencil. Our stencil is a minor extension of the multi-dimensional unstructured stencil of Ref. [10] and is formed by decomposing polytopal cells into triangular (2D) or tetrahedral (3D) substructures. This gives rise to a number of geometrical entities depicted in Fig. 2. In 3D, the various control positions p, z, f, and e denote respectively points (or nodes), zones (or cells), faces, and edges. In 2D, also depicted in Fig. 2, the face and edge control positions are degenerate.

The *iota* is the smallest letter in the Greek alphabet, and will be used to denote the smallest simplex definable with this set of control positions $\{p, z, f, e\}$. Depending upon the dimensionality, the iota is bounded by one of each of the types of control positions. The stencil also includes connectivity to adjacent iotas. The cell *corner* c consists of those iotas sharing a common z and p.

In the discrete equations, it will be necessary to refer to physical quantities in relation to the iota connectivity structure. The iota will be indicated by a superscript. The logical location of the variable relative to a particular iota is identified with a subscript. For example, $\mathbf{u}_z^i$ and $\mathbf{u}_p^i$ denotes velocity at cell center and point respectively relative to iota i, while σ_z^i and σ_p^i denote the stress at the respective locations. A geometrical quantity associated with an iota is the outward directed surface normal $\mathbf{N}^i = N^i\hat{\mathbf{n}}^i$ with area N^i and direction $\hat{\mathbf{n}}^i$. Here we use a caret to indicate unit vectors.

Sums: It will be necessary to perform summations over iotas or other geometrical quantities. Considerable notational simplification is achieved if summations are expressed in terms of iotas. In summation expressions, superscripts will be